

## Ultra-stable $\text{Hg}^+$ trapped ion frequency standard†

J. D. PRESTAGE, R. L. TJOELKER,  
G. J. DICK and L. MALEKI

California Institute of Technology, Jet Propulsion Laboratory,  
4800 Oak Grove Drive, Bldg 298, Pasadena, California 91109, USA

(Received 7 June 1991)

**Abstract.** We report the development of a fieldable frequency standard based on  $^{199}\text{Hg}^+$  ions confined in a hybrid r.f./dc linear ion trap. This trap permits storage of large numbers of ions with reduced susceptibility to the second-order Doppler effect caused by the r.f. confining fields. A 160 MHz wide atomic resonance line for the 40.5 GHz clock transition is used to steer the output of a 5 MHz crystal oscillator to obtain a stability of  $2 \times 10^{-15}$  for 24 000 s averaging times. For longer averaging intervals, measurements are limited by instabilities in available hydrogen maser frequency standards. Measurements with 37 mHz linewidth for the  $\text{Hg}^+$  clock transition demonstrate that the inherent stability for this frequency standard is at least as good as  $1 \times 10^{-15}$ .

### 1. Introduction

Atomic frequency standards with high stability for averaging times  $\tau$  longer than 1000 s are necessary for a variety of astrophysical measurements and long baseline spacecraft ranging experiments. The millisecond pulsar, PSR 1937+27, shows stability in its rotational period that exceeds that of all man-made clocks for averaging times longer than 6 months. Comparison of this pulsar period with an Earth-based clock of stability  $1 \times 10^{-15}$  over averaging periods of 1 year may show the effects of very low frequency ( $\approx 1$  cycle per year) gravitational waves [1, 2]. Spacecraft ranging measurements across the solar system would be improved with clocks whose stabilities exceed  $1 \times 10^{-15}$  for averaging times of  $10^4$ – $10^5$  s. This clock performance would also improve gravitational wave searches in spacecraft ranging data.

The performance of microwave frequency standards in use today are summarized in figure 1 [2, 3]. For short-term stability ( $\tau < 150$  s) the JPL superconducting cavity maser shows stability as good as  $2 \times 10^{-15}$  for averaging times up to 2000 s (R. Wang, pers. comm. and [4]). Hydrogen masers are presently the most stable frequency standard for  $150 < \tau < 30\,000$  s and are the primary standard in use in JPL's deep space tracking system. For averaging times greater than 6 months the millisecond Pulsar PSR 1937+21 exceeds the stability of international timekeeping abilities at a level of 1–2 parts in  $10^{-14}$  [3]. For  $\tau > 10^6$  s, the most stable clock yet measured is the  $\text{Hg}^+$  ion standard based on  $2 \times 10^6$  ions confined in a r.f. Paul trap [2, 5]. The subject of the present paper is a linear ion trap based  $\text{Hg}^+$  frequency standard now being tested at the Frequency Standards Laboratory at JPL. Stability

† This work represents the results of one phase of research carried out at the Jet Propulsion Laboratory, California Institute of Technology, under a contract sponsored by the National Aeronautics and Space Administration.

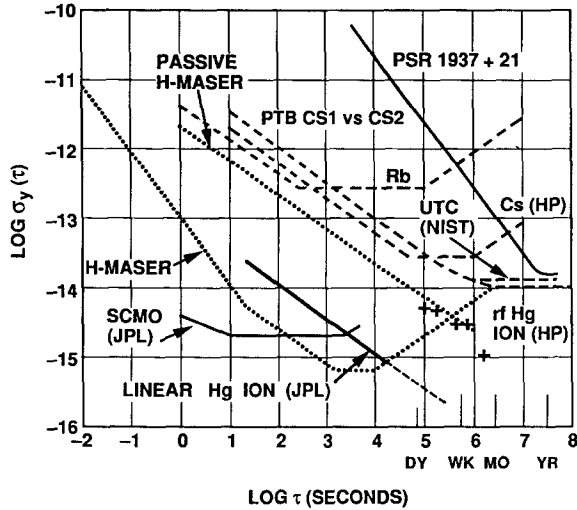


Figure 1. Fractional frequency stability of several precision frequency standards.

measurements of the  $\text{Hg}^+$  standard using an H-maser local oscillator are shown in figure 1. Determination of the long-term stability ( $\tau > 10\,000$  s) is limited by reference H-maser instabilities.

Typically, the largest source of frequency offset in standards based on ions confined in Paul traps stems from the motion of the ions caused by the trapping fields via the second-order Doppler or relativistic time-dilation effect. Though increasing ion number will lead to increasing signal to noise in the measurement of the clock transition, the frequency offset also grows with the number of ions, forcing a trade-off situation. Often fewer ions are trapped in order to reduce the (relatively) large offset and frequency instabilities that may result. For practical standards, such frequency offsets can be tolerated to the extent they can be stabilized.

## 2. Linear ion trap

In a conventional hyperbolic Paul trap, ions are trapped around a node of the r.f. electric field at the centre. The strength of the electric field and the resulting micromotion of the trapped particles grow linearly with distance from this node point. As ions are added the size of the ion cloud grows until the second-order Doppler shift arising from the micromotion in the trapping field dominates the second-order Doppler shift from the ion's thermal motion at ambient temperature. For typical operating conditions [6], a spherical cloud containing  $2 \times 10^6$  mercury ions shows a second-order Doppler shift of  $2 \times 10^{-12}$ , a value some 10 times larger than that due to thermal motion alone. In order to increase the number of stored ions with no corresponding increase in second-order Doppler shift from ion micromotion, we proposed and developed a hybrid r.f./dc linear trap [7]. This trap confines ions along a line of nodes of the r.f. field, effectively providing the same capability as a large number of hyperbolic traps acting together. The trapping force transverse to the line of nodes is generated by the ponderomotive force as in conventional Paul traps, while the axial trapping force is provided by dc electric fields [7–10]. Unlike

conventional r.f. traps, this linear trap will hold positive or negative ions but not both simultaneously. A related trap that uses purely ponderomotive forces to confine charged particles is the racetrack trap [11, 12].

We can compare the second-order Doppler shift  $\Delta f/f$  generated by the trapping fields for a cloud of ions in these two type of traps, assuming that both traps are operated with the same r.f. trapping force as characterized by the ion secular frequency  $\omega$ . If the same number of ions  $N$  is held in both traps, the average distance from an ion to the node of the trapping field is greatly reduced in the linear trap. Since the distance from the node determines the magnitude of the r.f. trapping field, the second-order Doppler shift of an ion's clock frequency due to motion in the trapping field is reduced from that of a hyperbolic trap. If  $R_{\text{sph}}$  is the ion cloud radius in the hyperbolic trap and  $L$  is the ion cloud length in the linear trap, the Doppler shift in the two traps are related by [7]

$$\left(\frac{\Delta f}{f}\right)_{\text{lin}} = \frac{5}{3} \frac{R_{\text{sph}}}{L} \left(\frac{\Delta f}{f}\right)_{\text{sph}} \quad (1)$$

As more ions are added to the linear trap this shift will increase. It will equal that of the spherical ion cloud in a hyperbolic trap when

$$N_{\text{lin}} = \frac{3}{5} \frac{L}{R_{\text{sph}}} N_{\text{sph}} \quad (2)$$

Equations (1) and (2) are valid when the ion cloud radii,  $R_{\text{lin}}$  and  $R_{\text{sph}}$ , are much larger than the Debye length, which is the characteristic plasma density decay length at the ion cloud edge, and is about 0.4 mm for typical  $\text{Hg}^+$  ion plasmas used in frequency standard work [6].

In addition to its larger ion-storage capacity, the dependence of the second-order Doppler shift on trapping parameters in a linear trap is very different from that in a conventional Paul trap. For many ions in a Paul trap this shift is given by [6, 7]

$$\left(\frac{\Delta f}{f}\right)_{\text{sph}} = -\frac{3}{10c^2} \left(\frac{N\omega q^2}{4\pi\epsilon_0 m}\right)^{2/3} \quad (3)$$

where  $\omega$  is the secular frequency for a spherical ion cloud containing  $N$  ions, each with charge to mass ratio  $q/m$ ,  $c$  is the speed of light and  $\epsilon_0$  is the permittivity of free space. Ions in a long linear trap where end effects are negligible show a second-order Doppler shift from the motion generated by the r.f. confining field, given by [7]

$$\left(\frac{\Delta f}{f}\right)_{\text{lin}} = -\left(\frac{q^2}{8\pi\epsilon_0 mc^2}\right) \frac{N}{L} \quad (4)$$

where  $N/L$  is the linear number density of ions in the trap.

In contrast to the spherical case described in equation (3), this expression contains no dependence on trapping field strength, as characterized by  $\omega$ , and depends only on the linear ion density  $N/L$ . If, for example, the r.f. confining voltage increases and, consequently, the micromotion at a given point in space increases, the ion-cloud radius will decrease so that the second-order Doppler shift (averaged over the cloud) from ion micromotion remains constant. Similar statements can be made about variations in any parameter that affects the radial confinement strength [8].

The sensitivity of the finite length linear trap to variations in radial trapping strength (characterized by  $\omega$ ) is [8]

$$\frac{\delta\left(\frac{\Delta f}{f}\right)_{\text{lin}}}{\left(\frac{\Delta f}{f}\right)_{\text{lin}}} = -2 \frac{R_t}{L} \frac{\delta\omega}{\omega}, \quad (5)$$

and to variations in endcap voltage is

$$\frac{\delta\left(\frac{\Delta f}{f}\right)_{\text{lin}}}{\left(\frac{\Delta f}{f}\right)_{\text{lin}}} = 2 \frac{R_t}{L} \frac{\delta V_e}{V_e}, \quad (6)$$

where  $R_t$  is the trap radius. The Paul trap shows a corresponding sensitivity to trap field strength variations:

$$\frac{\delta\left(\frac{\Delta f}{f}\right)_{\text{sph}}}{\left(\frac{\Delta f}{f}\right)_{\text{sph}}} = -\frac{2}{3} \frac{\delta\omega}{\omega}. \quad (7)$$

A comparison of equations (5) and (7) shows the linear trap based frequency standard to be less sensitive to variations in trapping field strength than the Paul trap by a factor of  $3R_t/L$ . For the trap described in the next section, this factor is about 1/3.

### 3. Operation with H-maser local oscillator

Our linear trap is shown in figure 2. Ions are created inside the trap by an electron pulse along the trap axis which ionizes a neutral vapour of  $^{199}\text{Hg}$ . A helium buffer gas ( $10^{-5}$  torr) collisionally cools the ions to near room temperature. Resonance radiation (194 nm) from a  $^{202}\text{Hg}$  discharge lamp optically pumps the ions into the  $F=0$  hyperfine level of the ground state [13]. This UV light is focused on to the central 1/3 of the 75 mm-long ion cloud. The thermal motion of the ions along the length of the trap will carry all the ions through the light field, so that pumping is complete in about 1.5 s for typical lamp intensities.

To minimize stray light entering the fluorescence collection system this state selection light is collected in a Pyrex horn, as shown in figure 2. Placement of the  $\text{LaB}_6$  electron filament is also chosen to prevent light from entering the collection system. Its placement and relatively cool operating temperature, together with good filtering of the state selection/interrogation UV light in the input optical system, have allowed frequency standard operation without the use of a 194 nm optical bandpass filter in the collection arm. This triples data-collection rates, since such filters typically have about 30% transmission for 194 nm light.

Microwave radiation (40.5 GHz) propagates through the trap perpendicular to the trap axis, satisfying the Lamb-Dicke requirement that the spatial extent of the ion's motion along the direction of propagation of the microwave radiation be less than a wavelength. Radiation enters the trap region through the Pyrex horn (see figure 2) and propagates in the opposite direction to the UV state selection/interrogation light. This allows collection of atomic fluorescence in both directions

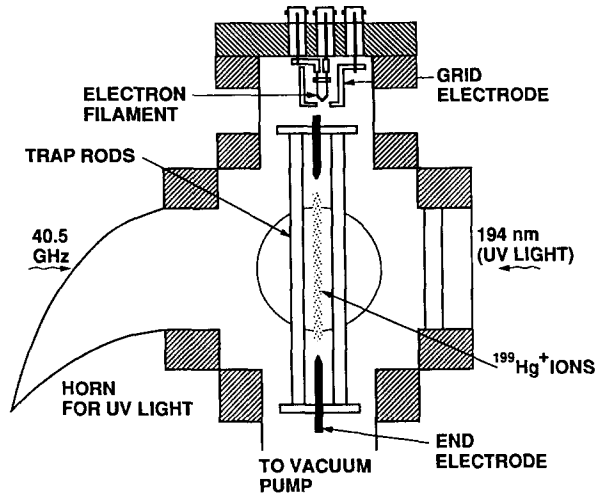


Figure 2. Linear ion trap assembly residing in its high vacuum enclosure. State selection light from the  $^{202}\text{Hg}$  discharge lamp enters from the right, is focused on to the central 1/3 of the trap and is collected in the horn. Fluorescence from the trapped ions is collected in a direction normal to the page.

perpendicular to the incident pumping light. For the resonance and stability data shown in this paper, fluorescence was collected in only one of these two directions.

At the present time no thermal regulation is incorporated into the ion standard itself. However, for all stability measurements described, the ion trap standard together with its support electronics were housed in an environmentally controlled test chamber where temperature variations were regulated to approximately  $\pm 0.05^\circ\text{C}$ . This level of regulation is much less demanding than that required, for example, by hydrogen masers.

We have used the technique of successive oscillatory fields [14] to probe the approximately 40.5 GHz hyperfine clock transition in  $^{199}\text{Hg}^+$  ions confined to the linear trap described above. In the initial measurements the 40.5 GHz signal is derived from an active hydrogen maser frequency source, as shown in figure 3. A representative resonance line of the  $^{199}\text{Hg}^+$  clock transition is shown in figure 4. State selection and interrogation is accomplished during the 1.5 s following the lamp turn on. It is necessary to switch the UV state selection/interrogation light level to near zero during the microwave interrogation period to prevent light shifts and broadening of the clock transition. A background light level of about 300 000 per 1.5 s collection period has been subtracted to generate the resonance shown. The successive oscillatory field pulses consist of two 0.35 s microwave pulses separated by a 2.5 s free precession period. The graph shown in figure 4 is an average of 10 scans, with a 10 MHz frequency step size.

The central portion of the narrowest resonance lines yet obtained with this apparatus is shown in figure 5. This line is derived from two 0.275 s pulses, separated by a 16.5 s free precession period [15]. The linewidth of 30 MHz represents a line  $Q$  of over  $1 \times 10^{12}$  on the 40.5 GHz transition. The graph displayed is an average of four full scans and, to our knowledge, is the highest  $Q$ -transition ever measured in a microwave atomic transition.

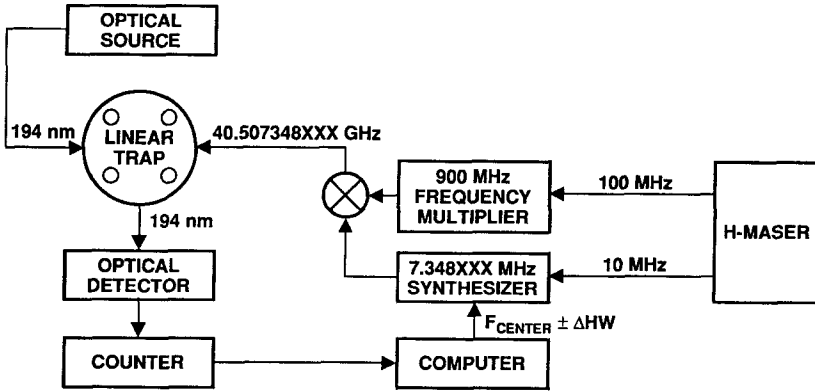


Figure 3. Schematic operation of the mercury ion trap using a hydrogen maser as the local oscillator.

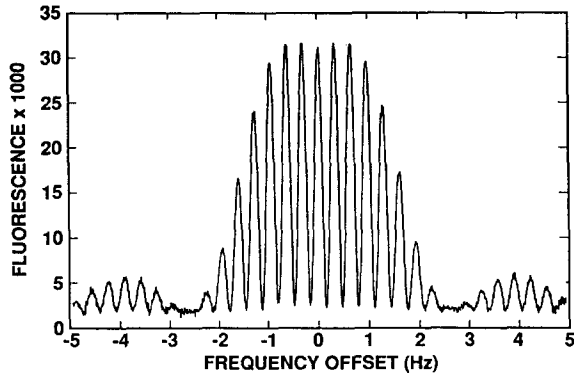


Figure 4.  $^{199}\text{Hg}^+$  clock transition, measured with method of successive oscillatory fields. This lineshape results from two 0.35 s microwave pulses separated by a 2.5 s free precession period. The central line is about 160 mHz wide and the data shown is an average of 10 scans.

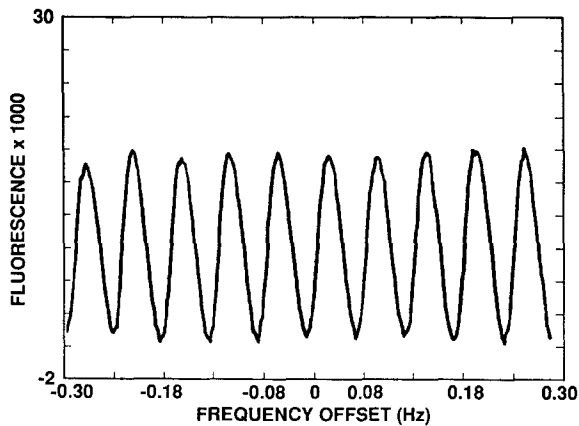


Figure 5. High  $Q$  Ramsey fringes resulting from two microwave pulses of 0.275 s separated by a 16 s free precession period. The fringes are about 30 mHz wide and the data shown is an average of four scans.

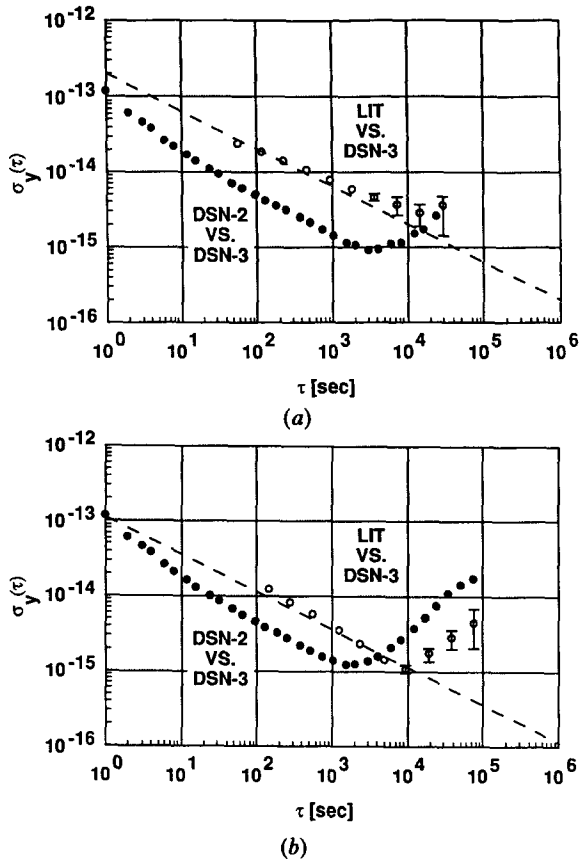


Figure 6. Performance of the Hg<sup>+</sup> system when the local oscillator (LO) is a hydrogen maser. The fractional frequency stability of the ion trap system is measured against an LO maser. (a) Stability obtained with a 160 mHz Hg<sup>+</sup> resonance line as shown in figure 4. The  $2 \times 10^{-13}/\sqrt{\tau}$  line is shown for reference. (b) Stability obtained with a 37 mHz Hg<sup>+</sup> resonance line. Also shown is the stability comparison of the LO maser with another H-maser.

To determine the frequency stability of the overall system of ions, trap, microwave source, etc., we have locked the output frequency of the 40.5 GHz source to the central peak of the 160 mHz resonance in a sequence of 16 384 frequency measurements. The time required for each measurement is about 7 s and the loop response time was five measurement cycles. By averaging the frequencies of  $2^N$  adjacent measurements ( $N=1, 2, \dots, 13$ ), we form the Allan deviation shown in figure 6 (a). Performance of the linear ion trap based Hg<sup>+</sup> standard measured in this manner is  $2 \times 10^{-13}/\sqrt{\tau}$  for averaging times  $\tau \leq 20\,000$  s, beyond which H-maser frequency instabilities limit the measurement. Figure 6 (b) shows better performance obtained with a 37 mHz wide resonance generated by two 0.35 s  $\pi/2$  pulses separated by a 13 s precession period. The stability measured in this mode of operation is  $1 \times 10^{-15}$  for a 10 000 s averaging time, as can be seen in the figure. Beyond 10 000 s, instability in the reference H-maser probably limits the measurement.

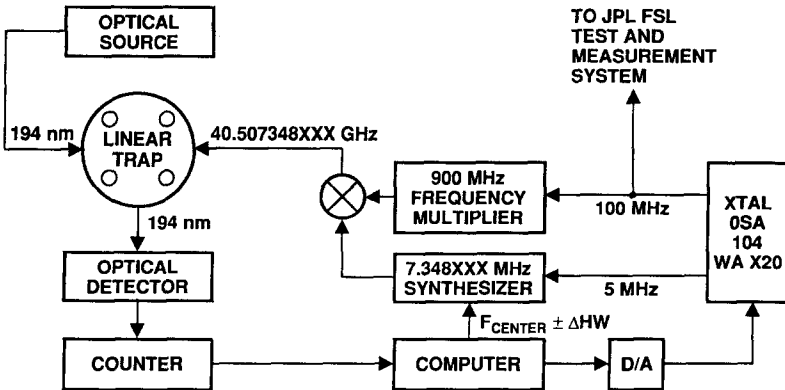


Figure 7. Schematic operation of the mercury ion trap to steer a quartz oscillator.

#### 4. Operation with a crystal oscillator

In this section we describe the long-term stability achieved when a commercial (Oscilloquartz 8600B No. 104) 5 MHz quartz crystal oscillator of superior performance is locked to the 160 mHz  $\text{Hg}^+$  ion resonance in figure 4. The schematic of this system is shown in figure 7. Using the JPL Frequency Standards Lab measurement system we have carried out a frequency stability measurement of the  $\text{Hg}^+$  steered crystal using two H-masers in the measurement system (designated DSN-2 and DSN-3) as references.

The results of this 63 h comparison are shown in figures 8 (a) and (b). The first figure shows the Allan deviation of the  $\text{Hg}^+$  steered crystal as measured against DSN-2 (upper trace) and against DSN-3 (lower trace). For averaging times less than 10 s the Allan deviation is that of the unsteered crystal oscillator, since the loop attack time is about 10 s. For averaging times shorter than about 13 000 s the  $\text{Hg}^+$  standard shows the same stability, independent of reference maser. For  $\tau > 20\,000$  s the Allan deviation of the  $\text{Hg}^+$  versus DSN-2 is the same as that for DSN-2 versus DSN-3 (see figure 8 (b)), indicating that DSN-2 has the limiting performance of the three standards under test for this averaging time period. The lower trace of figure 8 (a) shows a  $\text{Hg}^+$  standard stability of  $2 \times 10^{-15}$  for  $\tau = 24\,000$  s beyond which instabilities in DSN-3 probably limit the measurement. A second  $\text{Hg}^+$  ion standard is now under construction which will enable stability measurements beyond 24 000 s.

#### 5. Local oscillator considerations

Fluctuations in the local oscillator (LO) limit performance of a trapped ion standard in two ways. As discussed above, slow variations of the crystal LO are compensated by action of the servo system. The effectiveness of this compensation increases with the measuring time, so that for longer measuring times performance approaches the  $1/\sqrt{\tau}$  dependence, which is characteristic of passive standards. This behaviour is clearly shown in figure 8 (a).

However, fast fluctuations in the LO also degrade performance of the standard by an effect that adds to the (white) fluctuation of the photon count from measurement to measurement [16–18]. This limitation continues to the longest times, having the same  $1/\sqrt{\tau}$  dependence on measuring time  $\tau$  as the inherent performance of the

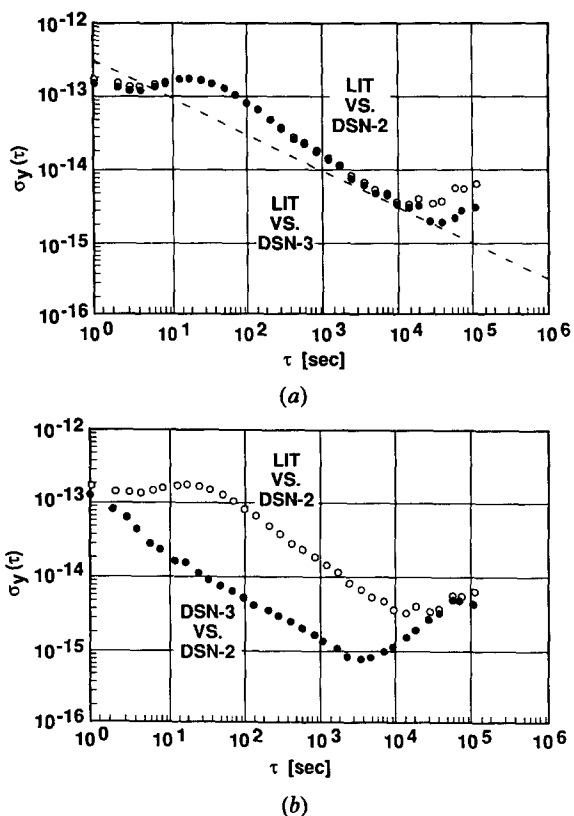


Figure 8. Performance of the  $Hg^+$  system when the LO is a quartz oscillator. (a) The ion trap standard compared with each maser independently distinguishes the different performance of the two masers for times  $\tau \geq 10\,000$  s. The dashed line represents the calculated  $1/\sqrt{\tau}$  performance based on actual operating conditions. (b) Fractional frequency stability compared with the hydrogen maser DSN-2, and maser comparison between DSN-2 and DSN-3.

standard itself. The cause of this effect can be traced to a time-varying sensitivity to LO frequency that is inherent in the interrogation process. This limitation was evaluated in a recent calculation for several types of sequentially interrogated passive standards [18].

Using this same methodology, we have calculated the LO-induced performance degradation for our particular interrogation scenario. Here, two r.f. pulses of 0.35 s length are separated by a delay of 2.5 s. A dead time of 3.8 s follows, to give the cycle time of  $t_c = 7$  s. Our quartz LO shows flicker frequency noise with an approximately flat Allan deviation of  $1.5 \times 10^{-13}$ . For this LO we calculate a contribution to the Allan deviation of the trapped ion source of  $2.6 \times 10^{-13}/\sqrt{\tau}$ . This value is slightly larger than the  $2.0 \times 10^{-13}/\sqrt{\tau}$  due to random fluctuations in the photon count, again based on actual operating conditions. The two contributions can be combined to give a limiting stability of  $3.3 \times 10^{-13}/\sqrt{\tau}$ , which is plotted along with the data in figure 8(a). The data confirm this analysis by a very close approach to the line for measuring times  $\tau > 10^3$  s.

Both LO and intrinsic statistical performance limitations may be reduced by increasing the interrogation time, as long as the dead time is not increased. The

implicitly higher  $Q$  and reduced (relative) dead time would result in a comparable improvement for each of the two contributions. For example, an increase in the interrogation time by four times would reduce the limiting  $1/\sqrt{\tau}$  Allan deviation by a half.

However, it is clear that as performance improves to make possible trapped ion performance in the low  $10^{-14}/\sqrt{\tau}$  range, quartz crystal LO performance will not be sufficient in itself to keep pace. In this case, a cryogenic LO with  $10^{-14}$  type stability for short times could be used, or a quartz LO with alternatively interrogated traps to give a uniform servo sensitivity with time [18].

## 6. Sources of frequency instability

While short-term performance of the ion trap standard is determined by the signal-to-noise ratio and the line  $Q$  of the clock transition resonance, the long-term stability is determined by the sensitivity of the atomic system to changes in environmental and operating parameters and on our ability to control and stabilize such parameters. The largest measured offsets of the  $\text{Hg}^+$  clock transition frequency under present operating conditions are shown in figure 9. When these offsets are stable the device serves as a practical frequency standard. In addition, when these offsets are quantified, the standard can achieve accuracy well below the magnitude of the frequency offsets.

The second-order Doppler shift from ion motion driven by the trapping field is determined by measuring the clock frequency as the ion number,  $N$ , decays during the approximately 2000 s ion-storage time for our trapping conditions. The frequency offset between our current operation with about  $5 \times 10^7$  ions and very few ions where trapping field shifts are minimized is  $1.5\text{--}2.0 \times 10^{-12}$ . No active ion number stabilization was used in any of the measurements described here though some stabilization is achieved by filling the trap to saturation level for the given dc voltage on the end electrodes. Saturation occurs so long as the net rate of ion generation in the trap is much higher than the ion loss rate. This present procedure is sufficient to maintain ion number stability of at least 0.1% over the 24 000 s averaging time required to reach  $2 \times 10^{-15}$  stability.

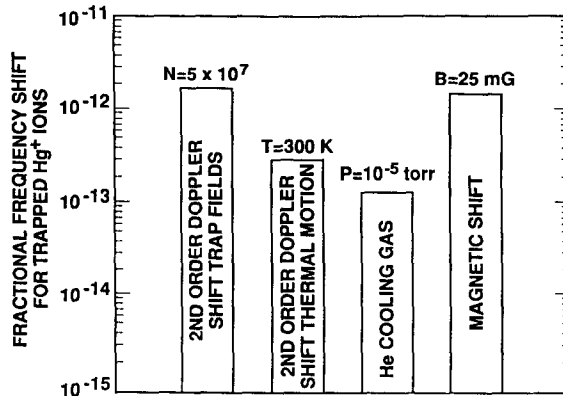


Figure 9. The largest measured perturbations to the  $^{199}\text{Hg}^+$  clock transition in the linear trap, under typical operating conditions.

The fractional sensitivity of the <sup>199</sup>Hg<sup>+</sup> clock transition to magnetic field variations is nearly 1000 times less than that of hydrogen at the same operating field. For the present measurements the field was set at 3.5 μT (35 mG). At this operating field the unshielded atomic sensitivity is  $1.7 \times 10^{-13} \text{ mG}^{-1}$ . To reach  $1 \times 10^{-16}$  frequency stability the current in the Helmholtz field bias coils must be stable to  $2 \times 10^{-5}$ . To prevent ambient field disturbances from influencing the ion frequency, the trap region is surrounded by a triple-layer magnetic shield of shielding factor 10 000. With this shielding factor, a 5 mG ambient field change would lead to a  $1 \times 10^{-16}$  shift in the atomic resonance frequency. Magnetic gradients must also be minimized in order to reach the highest frequency stability since gradients over the ion cloud can degrade atomic coherence and limit line  $Q$ . A partial solution has been to operate the standard at relatively high field settings (35 mG) but this also increases the atomic sensitivity to fluctuations in ambient field.

The fractional temperature sensitivity of the complete system is found to be less than  $10^{-14}/^\circ\text{C}$  which probably comes about via an increase in neutral mercury vapour and a consequent heating and/or ion cloud radius increase. The lamp and its housing must also be temperature-controlled as the brightness is highly dependent on temperature.

Long-term stability requires controlling these parameters to high precision. Since the mercury atom is, in general, less sensitive to environmental changes than other atoms used in frequency standards, an order of magnitude improvement may be obtained in long-term stability with the same level of control as existing standards.

## 7. Conclusions

By steering a 5 MHz crystal oscillator to a 160 mHz atomic resonance ( $Q = 3.3 \times 10^{11}$ ) we have measured performance of  $2 \times 10^{-15}$  for  $\tau = 24\,000$  s limited only by the stability of available reference hydrogen masers. While using a hydrogen maser as a local oscillator we have measured an Allan deviation of  $1 \times 10^{-15}$  at 10 000 s with a 37 mHz resonance line. Line  $Q$  values as high as  $1.3 \times 10^{12}$  have been measured [15], indicating consequent performance for this trap as good as  $5 \times 10^{-14}/\sqrt{\tau}$  for  $\tau > 150$  s.

## Acknowledgment

We wish to thank Randy Berends for making <sup>202</sup>Hg lamps and Bill Diener, Albert Kirk and Roland Taylor for assistance with the Frequency Standards Laboratory Test and Measurement System.

## References

- [1] DAVIS, M. M., TAYLOR, J. H., WEISBERG, J. M., and BACKER, D. C., 1985, *Nature*, **315**, 547.
- [2] ALLAN, D. W., WEISS, M. A., and PEPPLER, T. K., 1989, *IEEE Trans. Instrum Meas.*, **38**, 624.
- [3] RAWLEY, L. A., TAYLOR, J. H., DAVIS, M. M., and ALLAN, D. W., 1987, *Science*, **238**, 761.
- [4] WANG, R. T., and DICK, G. J., 1990, *Proc. 44th Ann. Symp. on Freq. Control, IEEE Cat. No. 87-654207*, p. 89.
- [5] CUTLER, L. S., GIFFARD, R. P., WHEELER, P. J., and WINKLER, G. M. R., 1987, *Proc. 41st Ann. Symp. Freq. Control, IEEE Cat. No. 87CH2427-3*, p. 12.
- [6] CUTLER, L. S., GIFFARD, R. P., and MCGUIRE, M. D., 1985, *Appl. Phys. B*, **36**, 137.

- [7] PRESTAGE, J. D., 1988, OSTDS Advanced Systems Review, JPL Internal Report, DSN RTOP 310-10-62, 14–15 June, p. 64; PRESTAGE, J. D., DICK, G. J., and MALEKI, L., 1989, *J. Appl. Phys.*, **66**, 1013.
- [8] PRESTAGE, J. D., JANIK, G. R., DICK, G. J., and MAEKI, L., 1990, *IEEE Trans. Ultrason. Ferroelec. Freq. Contr.*, **37**, 535.
- [9] JANIK, G. R., PRESTAGE, J. D., and MALEKI, L., 1990, *J. Appl. Phys.*, **67**, 6050.
- [10] WINELAND, D. J., BERGQUIST, J. C., BOLLINGER, J. J., ITANO, W. M., HEINZEN, D. J., GILBERT, S. L., MANNEY, C. H., and RAIZEN, M. G., 1990, *IEEE Trans. Ultrason. Ferroelec. Freq. Contr.*, **37**, 515.
- [11] DEHMELT, H. G., 1989, *Proc. 4th Symp. Frequency Standards and Metrology*, p. 286.
- [12] CHURCH, D. A., 1969, *J. Appl. Phys.*, **40**, 3127.
- [13] MAJOR, F. G., and WERTH, G., 1981, *Appl. Phys.*, **15**, 201.
- [14] RAMSEY, N. F., 1956, *Molecular Beams* (Oxford: Oxford University Press).
- [15] PRESTAGE, J. D., DICK, G. J., and MALEKI, L., 1991, *IEEE Trans. Instrum. Meas.*, **40**, 132.
- [16] DICK, G. J., 1988, *Proc. 19th Ann. Precise Time and Time Interval (PTTI) Applications and Planning Meeting*, p. 133.
- [17] AUDOIN, C., CANDELIER, V., and DIMARCO, N., 1991, *IEEE Trans. Instrum. Meas.*, **40**, 121.
- [18] DICK, G. J., PRESTAGE, J. D., GREENHALL, C. A., and MALEKI, L., 1990, *Proc. 22nd Ann. Precise Time and Time Interval (PTTI) Applications and Planning Meeting*, p. 487.